Systematic study of the surface properties of the nuclear potential with high precision large-angle quasi-elastic scatterings

C. J. Lin, H. M. Jia,* H. Q. Zhang, F. Yang, X. X. Xu, F. Jia, and Z. H. Liu
China Institute of Atomic Energy, P. O. Box 275(10), Beijing 102413, People's Republic of China

K. Hagino
Department of Physics, Tohoku University, Sendai 980-8578, Japan
(Received 3 April 2009; published 11 June 2009)

High precision excitation functions of large-angle quasi-elastic scattering for the systems of $^{16}O + ^{208}Pb$, ^{196}Pt, ^{184}W, and $^{154,152}Sm$ at energies well below the Coulomb barrier were measured. The surface diffuseness parameters of the real part of the Woods-Saxon potential have been extracted from the single-channel and coupled-channels calculations, respectively. By considering the effect of couplings, the extracted diffuseness parameters are in the range from 0.64 to 0.69 fm, which is close to the values extracted from the systematic analyses of elastic and inelastic scattering data. On the other hand, single-channel calculations give somewhat larger values in the range from 0.68 to 0.77 fm, especially for systems with deformed target nuclei.

DOI: 10.1103/PhysRevC.79.064603 PACS number(s): 25.70.Bc, 24.50.+g

I. INTRODUCTION

The optical potential has been extensively used in the analyses of heavy-ion reactions. In these analyses, the Woods-Saxon (WS) potential inside the Coulomb barrier is not completely clear. Recently, Newton *et al*. [1] found that the large diffuseness parameters of the WS potential in the range from 0.75 to 1.5 fm were required to fit a number of precise fusion excitation functions at energies above the average fusion barriers. The result shows that the diffuseness parameters are obviously greater than the commonly accepted value of 0.63 fm from the systematic analyses of elastic and inelastic scattering data [2–5]. The reason for the large discrepancy in the diffuseness parameters extracted from scattering and fusion analyses is still unknown.

Quasi-elastic scattering and fusion are both inclusive processes and are complementary to each other. Consequently these reactions undergo the same potential and share the same information on the reaction mechanism. Therefore, quasi-elastic scattering can also be used to study the nuclear potential. It is just similar to studying the fusion barrier distribution from the excitation function of quasi-elastic scattering near the barrier energies. Recently, large-angle quasi-elastic scattering has been used to study the nuclear potential [6–11]. Washiyama *et al*. [7] carried out a systematic analysis of the surface diffuseness parameter with this method. The result shows that a surface diffuseness parameter of about 0.6 fm is needed to fit the quasi-elastic scattering data for the spherical reaction systems, while a larger diffuseness parameter of 0.8–1.1 fm is favored for the deformed reaction systems. Unfortunately, the experimental data were not precise enough for this purpose.

Very recently, a few high precision experiments were performed to study this subject. Gasques *et al*. [8] performed a systematic study of the surface diffuseness parameter by using the measured high precision sub-barrier quasi-elastic scattering at a backward angle for a number of reactions whose Z_pZ_t is around 1200. The optimal single-channel and coupled-channels fitting to the experimental data were used with a diffuseness parameter of about 0.75 fm for near-spherical nucleus systems. But for deformed nucleus systems, coupled-channels calculations are important even at deep sub-barrier energies. In general, the effect of couplings is to make the quasi-elastic scattering cross sections drop more rapidly with increasing energy as compared with the single-channel calculation. The coupled-channels calculations resulted in a weighted average diffuseness parameter of 0.70 ± 0.01 fm for all the measured reactions. Evers *et al*. [9] have also reached a similar result.

In addition, Hinde *et al*. [12] have skillfully used the oscillatory quasi-elastic Mott scattering at near-barrier energies to determine the surface diffuseness parameter for a symmetric system. For the collisions of identical nuclei, the presence of nuclear potential will slightly alter the angular separation of Mott peaks in the angular distribution. For the $^{58}Ni + ^{58}Ni$ system, the extracted diffuseness parameter is 0.62 ± 0.04 fm by matching the experimental peak angles.

In this paper, we will show our main experimental results and consider the effect of the couplings to the different intrinsic states in the spherical and well-deformed systems. Spherical (^{208}Pb), short-elliptical (^{196}Pt), and long-elliptical (^{184}W, $^{154,152}Sm$) target nuclei were included in our study. The high precision cross sections of quasi-elastic scattering at a backward angle were measured with a statistical error of about 0.4%, at energies ranging from 0.50 to 1.00 of the respective fusion barriers V_B. The main purpose of this work is to obtain the diffuseness parameters of the real part of the WS potential with a consistent analysis for these reaction systems. Therefore, this study can be regarded as a complementary work of Gasques *et al*. [8] and of Evers *et al*. [9].

II. EXPERIMENTAL PROCEDURE

The experiment was performed at the HI-13 tandem accelerator of the Beijing Tandem Accelerator National Laboratory of the China Institute of Atomic Energy. A collimated ^{16}O

*Corresponding author: jiahm@ciae.ac.cn

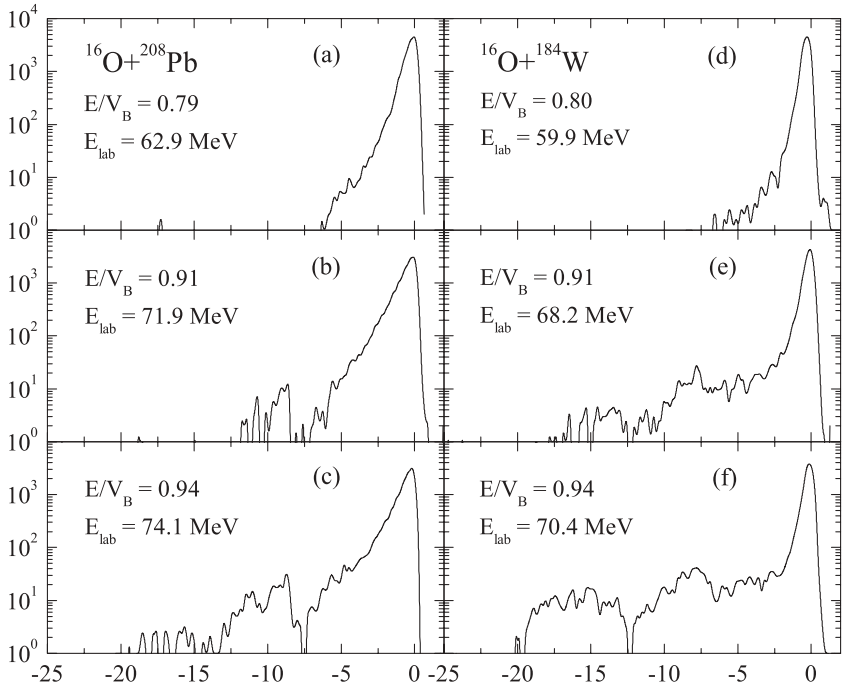

FIG. 1. Energy spectra measured at $\theta_{lab} = 175^\circ$ for the $^{16}O + ^{208}Pb$ and $^{16}O + ^{184}W$ reactions.

beam with incident energies in the range from 36 to 80 MeV bombarded the targets. The bombarding energies were varied in steps of 3 MeV at the very low energies and in steps of 0.68 MeV at the high energies. The isotopically enriched thin targets (100–200 μg/cm^2 thickness) of ^{208}Pb, ^{196}Pt, ^{184}W, and ^{154,152}Sm with a diameter of 3 mm were evaporated onto 20 μg/cm^2 carbon backings.

Two collimators were mounted in the entrance and exit tubes about 110 cm apart from each other. The scattered particles were detected by four Si(Au) surface-barrier detectors located at 175° relative to the beam direction. Four Si(Au) monitor detectors (up and down, left and right) located at the angle 41° with respect to the beam direction were used to detect the elastic scattering particles for normalization, also used to check the beam quality and to correct the beam direction. The relative solid angles subtended by the semiconductors were determined by using a ^{241}Am α source. In order to reduce the magnetic hysteresis, the beam energy was monotonically increased in the experiment. At some energies, the measurements were repeated to make sure that the response of the detectors did not deteriorate during the experiment. The data points measured at sufficiently low energies were found to be insensitive to the nuclear potential, and thus were used for a reliable normalization to the Rutherford cross section. However, the variation in the axial position of the different targets, due to variations of the target mounting and planarity, results in slight differences in the normalization factor of $d\sigma_{qel}/d\sigma_{Ru}$ between the various targets.

The typical spectra of the $^{16}O + ^{208}Pb$ and $^{16}O + ^{184}W$ reactions at $\theta_{lab} = 175^\circ$ for three below-barrier energies are shown in Fig. 1. It can be seen that more exit channels emerge with the increasing energy besides the elastic scattering for the systems, despite of somewhat bad energy resolution partly due to a lack of a perfect uniformity of the targets. For $E/V_B = 0.94$ spectra, two groups of peaks concentrated roughly at -8 and -16 MeV may be caused by the direct transfer or deep-inelastic reactions for the $^{16}O + ^{184}W$ system, but for the $^{16}O + ^{208}Pb$ system only one group is visible. The quasi-elastic events were defined as the sum of the elastic and all the other direct constituents at lower energies in each spectrum. The background counts in the spectra are almost nonexistent due to the collimator in the exit tube, which limits the back-scattering products from the Faraday cup into the backward detectors.

III. DATA ANALYSIS AND RESULTS

The single channel and coupled-channels calculations were preformed with a modified version of the code CCFULL [13] for quasi-elastic scattering with a nuclear potential of WS form. Following the procedure of Ref. [9], an imaginary potential with $W = 30$ MeV, $a_w = 0.1$ fm, and $r_w = 0.8$ fm, which was well kept inside the Coulomb barrier, was chosen to represent the rather small absorption from barrier penetration in the calculations. This short-range imaginary potential does not influence the quasi-elastic scattering cross section predictions because its strength at the surface region is negligible.

Considering the real part of the nuclear potential, the surface diffuseness parameter can be determined unambiguously due to the compensative effect of the variations in both the V_0 and r_0 values on the Coulomb barrier height energy at the surface region. The parameters of the real part of WS potential were searched for the optimal fitting to the quasi-elastic scattering data. At the same time, the expected energy of the average fusion barrier height should be reproduced in the calculations. The fusion barrier height energies are listed in Table I which are taken from Ref. [1] or determined by using the Coulomb scaling parameter $Z_pZ_t/(A_p^{1/3} + A_t^{1/3})$ from the adjacent reaction systems. Of course, the reasonable change of fusion barrier

TABLE I. The fusion barrier height energies used to determine the real part of the nuclear potential in the calculations.

Reaction	V_B (MeV)	Method of determination
$^{16}O + ^{208}Pb$	74.52	Ref. [1]
$^{16}O + ^{196}Pt$	71.37	Scaled from the $^{16}O + ^{194}Pt$ data
$^{16}O + ^{184}W$	69.04	Scaled from the $^{16}O + ^{186}W$ data
$^{16}O + ^{154}Sm$	59.35	Ref. [1]
$^{16}O + ^{152}Sm$	59.53	Scaled from the $^{16}O + ^{154}Sm$ data

energy has only little influences on the extracted diffuseness parameters. For consistency, $V_0 = 100$ MeV for both single-channel and coupled-channels calculations were used for all the reactions. $V_0 = 100$ MeV is comparatively close to the potential depths of the Woods-Saxon parametrization of the exponential Akyüz-Winther potential, which was derived from a least-squares fit to experimental elastic scattering data, and therefore may be preferable for the description of peripheral reactions. For fixed V_0, r_0 and a values of the real part potential parameters were searched for the best fitting data. In the coupled-channels calculations, the minor difference of the r_0 parameter due to potential renormalization [14,15] compared with the single-channel calculation could be omitted because of its insensitivity on the derived diffuseness parameter [9].

In the calculations, the couplings to the first 3^- state in ^{16}O only slightly influence the extracted diffuseness parameter. Therefore, the inelastic excitations of ^{16}O were not included in the coupled-channels calculations for all of the measured reactions. Details of the collective states of the target nuclei included in the coupled-channels calculations are given thereafter for each reaction. The coupling of the transfer reaction is not included in the present calculations. According to the procedure mentioned in Ref. [7], only those experimental data for each reaction, in which the ratios of the quasi-elastic to the Rutherford cross sections are larger than around 0.94, were used in the following analyses. The uncertainties on the diffuseness parameters were assessed by increasing the minimum χ^2/N value plus 1, while keeping all other parameters fixed.

A. The $^{16}O + ^{208}Pb$ reaction

The measured excitation function of quasi-elastic scattering for the $^{16}O + ^{208}Pb$ system at $\theta_{lab} = 175^\circ$ is shown in Fig. 2. The energies have been corrected for the target thickness and converted to the center-of-mass system. The solid curve in the figure indicates the best-fit result using the single-channel potential with diffuseness parameter $a = 0.69 \pm 0.02$ fm.

The experimental excitation function was also compared with the coupled-channels calculations taking into account the 3^- and 5^- states in ^{208}Pb with corresponding excitation energies $\epsilon_3 = 2.615$ and $\epsilon_5 = 3.198$ MeV, respectively. The deformation parameters were taken as $\beta_3 = 0.122$ and $\beta_5 = 0.08$ following Ref. [16]. The diffuseness parameter giving the best fit to the experimental data does not differ much from the one obtained by using a single-channel calculation. The result is illustrated by the dashed curve in Fig. 2. The values of the diffuseness parameter obtained by the single-channel and coupled-channels analyses are in good agreement with each other, and also similar to the extracted result in Ref. [9]. As expected, the effect of couplings has only a minor influence on the quasi-elastic reactions involving spherical nuclei at deep sub-barrier energies, and this small effect can be neglected.

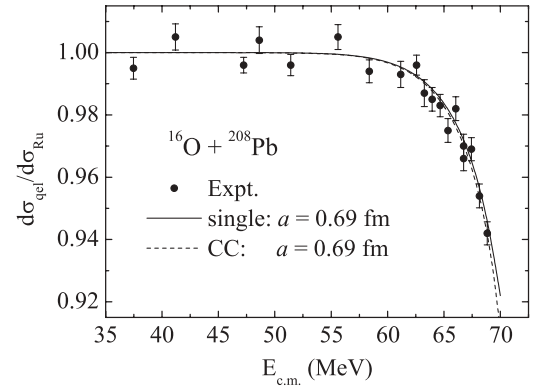

FIG. 2. The ratio of the quasi-elastic scattering to the Rutherford cross section measured at $\theta_{lab} = 175^\circ$ for the $^{16}O + ^{208}Pb$ reaction varies with the center-of-mass energy. The solid and dashed curves represent the optimal fitting results obtained from single-channel and coupled-channels calculations.

B. The $^{16}O + ^{196}Pt$ reaction

Figure 3 shows the measured excitation function of quasi-elastic scattering for the $^{16}O + ^{196}Pt$ reaction. The solid line was calculated by using a single-channel potential with $a = 0.68 \pm 0.02$ fm, which corresponds to the best χ^2 fit to the data.

In the coupled-channels calculations, the three lowest rotational states of the target nucleus with a β_2 deformation parameter of -0.138 [17] were included. With the couplings, the optimal fitting excitation function with the diffuseness parameter $a = 0.65 \pm 0.02$ fm is indicated by the dashed line in Fig. 3. It can be seen from this figure that the single-channel and coupled-channels calculations give almost the same results despite slightly different values for the diffuseness parameters.

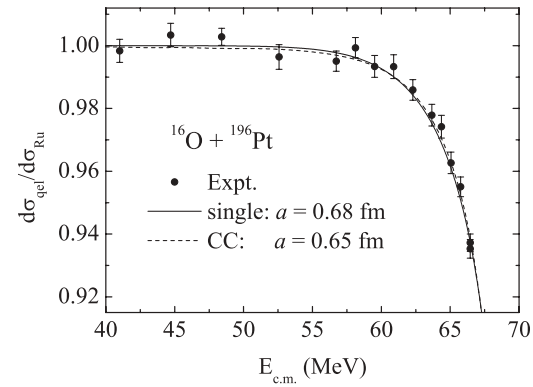

FIG. 3. Same as Fig. 2, but for the $^{16}O + ^{196}Pt$ system.

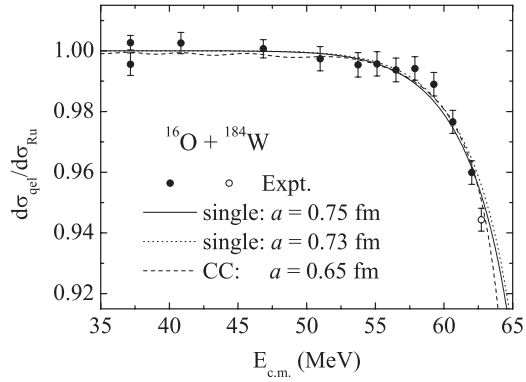

FIG. 4. Same as Fig. 2, but for the $^{16}O + ^{184}W$ system. The dotted curve is the single-channel calculation result with $a = 0.73$ fm.

C. The $^{16}O + ^{184}W$ reaction

The measured excitation function of quasi-elastic scattering for the $^{16}O + ^{184}W$ system is shown in Fig. 4. In the coupled-channels analysis, rotational couplings for ^{184}W were included, in which a total of five rotational states were considered with β_2 and β_4 deformation parameters of 0.262 and −0.189 [18]. The best description of the quasi-elastic scattering data is obtained with $a = 0.65 \pm 0.02$ fm as shown in Fig. 4 by the dashed line.

The solid line in the figure indicates the result of the best-fitting single-channel nuclear potential with a larger diffuseness parameter $a = 0.75 \pm 0.03$ fm. If the highest energy point (open circle in the figure) is excluded, the optimal fit result with a reduced $a = 0.73 \pm 0.04$ fm is shown in Fig. 4 by the dotted line. As soon as the point of data is progressively excluded in the fitting, some information on coupling and absorption effects may be extracted with an even smoother quasi-elastic scattering excitation function.

D. The $^{16}O + ^{154,152}Sm$ reactions

The measured quasi-elastic scattering excitation function for the $^{16}O + ^{154}Sm$ system is shown in Fig. 5(a). In the coupled-channels analysis, a total of five rotational states with deformation parameters $\beta_2 = 0.304$ and $\beta_4 = 0.052$ [19] for ^{154}Sm were used in the calculations. The best fitting excitation function with the diffuseness parameter of $a = 0.64 \pm 0.02$ fm is presented by the dashed curve in Fig. 5(a). Executing a single-channel analysis, the best fitted value with $a = 0.75 \pm 0.03$ fm is shown in Fig. 5(a) by the solid curve. This is in good agreement with the result in Ref. [9].

The same analysis was preformed for the $^{16}O + ^{152}Sm$ system. As shown in Fig. 5(b), the minimum χ^2/N value was reached using $a = 0.77 \pm 0.02$ fm and 0.64 ± 0.02 fm in the single-channel and coupled-channels calculations with the relevant deformation parameters $\beta_2 = 0.280$ and $\beta_4 = 0.092$ [20] for ^{152}Sm, respectively. The calculation results are almost the same for the two systems due to the very similar properties of the targets.

It can be seen from the figure that the fitting results with single-channel and coupled-channels calculations appear different. The coupled-channels calculations give a smaller

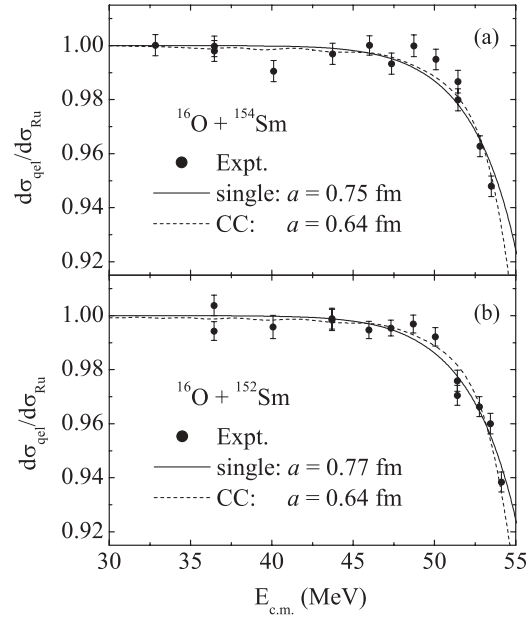

FIG. 5. Same as Fig. 2, but for the $^{16}O + ^{154}Sm$ system (a) and for the $^{16}O + ^{152}Sm$ system (b).

diffuseness parameter and a better description of the quasi-elastic data. The couplings change the shape of the quasi-elastic excitation function and make the better fitting even at deep sub-barrier energies. The diffuseness parameters extracted in this work are listed in Table II with uncertainties shown in parenthesis. For the deformed systems, the influence of the coupling effects on the quasi-elastic scattering arises with increasing quadrupole deformation parameters, without obvious relation to the deformation polarity.

IV. SUMMARY

In this work, the high-precision excitation functions of large-angle quasi-elastic scattering for the systems of $^{16}O + ^{208}Pb$, ^{196}Pt, ^{184}W, and $^{154,152}Sm$ at the deep sub-barrier energies were measured. Both single-channel and coupled-channels calculations have been used to analyze the data. Single-channel fitting quasi-elastic scattering data leads to diffuseness parameter a values in the range from 0.68 to 0.77 fm. While coupled-channels calculations result in a weighted average value for the diffuseness parameter of $a = 0.65 \pm 0.01$ fm for all the studied reactions. This value agrees

TABLE II. Diffuseness parameters extracted from the single-channel (SC) and coupled-channels (CC) calculations for all the studied systems. N is the number of the experimental data points.

Reaction	a^{SC} (fm)	χ^2/N	a^{CC} (fm)	χ^2/N
$^{16}O + ^{208}Pb$	0.69(0.02)	1.38	0.69(0.02)	1.21
$^{16}O + ^{196}Pt$	0.68(0.02)	0.63	0.65(0.02)	0.56
$^{16}O + ^{184}W$	0.75(0.03)	0.63	0.65(0.02)	0.58
$^{16}O + ^{154}Sm$	0.75(0.03)	1.91	0.64(0.02)	1.21
$^{16}O + ^{152}Sm$	0.77(0.02)	1.38	0.64(0.02)	1.50

with the theoretical calculation result using the double-folding potential model. This result further confirms that the effect of couplings influences significantly the quasi-elastic scattering for well-deformed nucleus systems even at deep sub-barrier energies. Being similar to the results of Ref. [9], no anomalous behavior of a large diffuseness parameter value exists when considering the coupled-channels effect in large-angle quasi-elastic scattering at deep sub-barrier energies. No strong effects were found for the opposite polarity of the quadrupole deformation parameter of the target nuclei. The complicated quasi-elastic energy spectrum below the barrier energies strongly hints that some dynamical processes have emerged at deep sub-barrier energies, but they were not included in the present coupled-channels calculations. So the complicated energy spectrum must be identified experimentally, and a refined self-consistent theory to depict the reaction processes at sub-barrier energies will have to be developed simultaneously.

ACKNOWLEDGMENTS

This work was supported by the National Natural Science Foundation of China under Grant Nos. 10575134, 10675169, 10735100, the Major State Basic Research Developing Program under Grant No. 2007CB815003, and the Japanese Ministry of Education, Culture, Sports, Science and Technology by Grant-in-Aid for Scientific Research under program no. 19740115.

[1] J. O. Newton, R. D. Butt, M. Dasgupta, D. J. Hinde, I. I. Gontchar, C. R. Morton, and K. Hagino, Phys. Rev. C **70**, 024605 (2004).
[2] P. R. Christensen and A. Winther, Phys. Lett. **B65**, 19 (1976).
[3] M. Lozano and G. Madurga, Nucl. Phys. **A334**, 349 (1980).
[4] L. C. Chamon, D. Pereira, E. S. Rossi Jr., C. P. Silva, H. Dias, L. Losano, and C. A. P. Ceneviva, Nucl. Phys. **A597**, 253 (1996).
[5] C. P. Silva, M. A. G. Alvarez, L. C. Chamon, D. Pereira, M. N. Rao, E. S. Rossi Jr., L. R. Gasques, M. A. E. Santo, R. M. Anjos, J. Lubian, P. R. S. Gomes, C. Muri, B. V. Carlson, S. Kailas, A. Chatterjee, P. Singh, A. Shrivastava, K. Mahata, and S. Santra, Nucl. Phys. **A679**, 287 (2001).
[6] K. Hagino, T. Takehi, A. B. Balantekin, and N. Takigawa, Phys. Rev. C **71**, 044612 (2005).
[7] K. Washiyama, K. Hagino, and M. Dasgupta, Phys. Rev. C **73**, 034607 (2006).
[8] L. R. Gasques, M. Evers, D. J. Hinde, M. Dasgupta, P. R. S. Gomes, R. M. Anjos, M. L. Brown, M. D. Rodríguez, R. G. Thomas, and K. Hagino, Phys. Rev. C **76**, 024612 (2007).
[9] M. Evers, M. Dasgupta, D. J. Hinde, L. R. Gasques, M. L. Brown, R. Rafiei, and R. G. Thomas, Phys. Rev. C **78**, 034614 (2008).
[10] O. A. Capurro, J. O. Fernández Niello, A. J. Pacheco, and P. R. S. Gomes, Phys. Rev. C **75**, 047601 (2007).
[11] D. S. Monteiro, J. M. B. Shorto, J. F. P. Huiza, P. R. S. Gomes, and E. Crema, Phys. Rev. C **76**, 027601 (2007).
[12] D. J. Hinde, R. L. Ahlefeldt, R. G. Thomas, K. Hagino, M. L. Brown, M. Dasgupta, M. Evers, L. R. Gasques, and M. D. Rodriguez, Phys. Rev. C **76**, 014617 (2007).
[13] K. Hagino, N. Rowley, and A. T. Kruppa, Comput. Phys. Commun. **123**, 143 (1999).
[14] K. Hagino, N. Takigawa, and S. Kuyucak, Phys. Rev. Lett. **79**, 2943 (1997).
[15] I. I. Gontchar, D. J. Hinde, M. Dasgupta, and J. O. Newton, Phys. Rev. C **69**, 024610 (2004).
[16] S. Santra, P. Singh, S. Kailas, A. Chatterjee, A. Shrivastava, and K. Mahata, Phys. Rev. C **64**, 024602 (2001).
[17] A. Sethi, N. M. Hintz, D. N. Mihailidis, A. M. Mack, M. Gazzaly, K. W. Jones, G. Pauletta, L. Santi, and D. Goutte, Phys. Rev. C **44**, 700 (1991).
[18] I. Y. Lee, J. X. Saladin, J. Holden, J. O'Brien, C. Baktash, C. Bemis Jr., P. H. Stelson, F. K. McGowan, W. T. Milner, J. L. C. Ford, Jr., R. L. Robinson, and W. Tuttle, Phys. Rev. C **12**, 1483 (1975).
[19] J. R. Leigh, N. Rowley, R. C. Lemmon, D. J. Hinde, J. O. Newton, J. X. Wei, J. C. Mein, C. R. Morton, S. Kuyucak, and A. T. Kruppa, Phys. Rev. C **47**, R437 (1993).
[20] L. K. Peker, Nucl. Data Sheets **58**, 93 (1989).